Micro–slips to 'Avalanches' in Confined, Molecular Layers of Ionic Liquids

ARTICLE *in* JOURNAL OF PHYSICAL CHEMISTRY LETTERS · DECEMBER 2013

Impact Factor: 7.46 · DOI: 10.1021/jz402451v

THE JOURNAL OF PHYSICAL CHEMISTRY Letters

Letter

pubs.acs.org/JPCL

Microslips to "Avalanches" in Confined, Molecular Layers of Ionic Liquids

R. M. Espinosa-Marzal,[†,§] A. Arcifa,[†] A. Rossi,[†,‡] and N. D. Spencer*[,†]

[†]Lab. for Surface Science and Technology, Dept. of Materials, ETH Zurich, Wolfgang-Pauli-Strasse 10, CH-8093 Zurich, Switzerland

[‡]Dipartimento di Scienze Chimiche e Geologiche, Università di Cagliari, S.S. 554 Bivio per Sestu, 09042 Cagliari, Italy

Supporting Information

ABSTRACT: We have measured forces between mica surfaces across two hydrophobic ionic liquids with a surface forces apparatus. Both surface-adsorbed water and alkyl-chain length on the imidazolium cation influence the structure of the nanoconfined film and the dynamics of film-thickness transitions. Friction shows accumulative microslips as precursors to collective "avalanches" that abruptly reduce friction momentarily. This behavior is interpreted as a consequence of interlayer ion correlations within the 1 to 2 nm thick film; we identify this to be analogous to the friction response of crackling noise systems over a broad range of sizes.

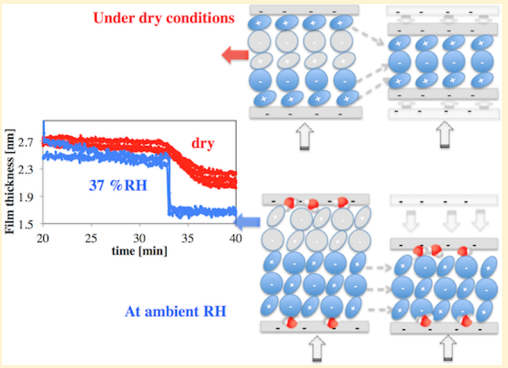

SECTION: Surfaces, Interfaces, Porous Materials, and Catalysis

Ionic liquids (ILs) are organic salts with melting points below 100 °C. ILs display high electrochemical and thermal stability, are nonflammable and nonvolatile,[1−3] and can be designed to interact with specific chemical groups, making them attractive in many applications including self-assembly media[4] and electrolytes for energy-storage systems.[1] Several studies have shown the layered structure of ILs in nanoconfinement[5−14] and how this can aid in reducing friction. Here we show the influence of IL composition on the stick−slip response upon shearing of 1 to 2 nm thin films with a very high time-scale resolution, revealing details of interlayer ion correlations. Stick−slip has often been measured in surface forces apparatus (SFA) experiments when sliding two atomically flat surfaces against each other, with a thin film acting as boundary lubricant (e.g., refs 15−18). This phenomenon has been explained through melting-freezing phase transitions of the lubricant molecules during continuous sliding, and the corresponding static and kinetic friction forces have been measured. We observe a nonperiodic stick−slip response and identify an analogy between this dynamic behavior and the response of crackling noise systems ranging over a broad range of sizes,[19,20] from slip avalanches in nanocrystals, through friction during bacterial motion, to earthquakes.

We present results obtained with two imidazolium-based ILs (Merck, purity >99%, water content <100 ppm): 1-hexyl-3-methyl imidazolium ($HMIM^+$) and 1-ethyl-3-methyl imidazolium ($EMIM^+$), both with the tris(pentafluoroethyl)-trifluorophosphate (FAP^-) anion, which renders the ILs hydrophobic (i.e., insignificant hydrogen bonding with water and dipole−dipole ion−water interactions). An extended surface forces apparatus (eSFA)[21−23] was used to explore normal and friction forces between mica surfaces across the selected ILs. A transmitted white-light interference spectrum is analyzed by fast-spectral-correlation interferometry to determine the gap distance and the refractive index simultaneously. Mica surfaces are prepared according to the usual protocol. (See the Supporting Information (SI) for more details about the experimental method and Figure S1 for the optimized geometry of the selected ions.)

A 10 μL droplet of vacuum-dried IL was deposited between the mica surfaces using a Hamilton syringe with a flat-end needle (model 710), during continuous purging of the eSFA cell with dry N_2. The cell was sealed, and the system was left to equilibrate for 3 h. Measurements were also performed at ambient RH (37 ± 2%) with an open eSFA cell and IL that was equilibrated at ambient RH. The water uptake by [EMIM] FAP and [HMIM] FAP (determined by coulometric Karl Fischer titration) at 37 ± 2% RH is 0.07 and 0.08% w/w, respectively, while the corresponding surface coverage of mica with water is 71.4%, that is, less than one monolayer.[24]

Force−distance curves were measured under dry conditions and at ambient RH by loading/unloading the surfaces at constant speed (0.08 to 0.3 nm/s). For the friction experiments, the lower surface was moved at 0.1 μm/s by means of a piezo bimorph with an amplitude of 10 μm, and shear forces

Received: November 13, 2013
Accepted: December 11, 2013
Published: December 11, 2013

were measured at a rate of 300 Hz (see SI for details). All measurements were performed at 22 °C.

Figure 1a shows the measured normal force versus thickness (D) of the confined [EMIM] FAP film in equilibrium at 0 and

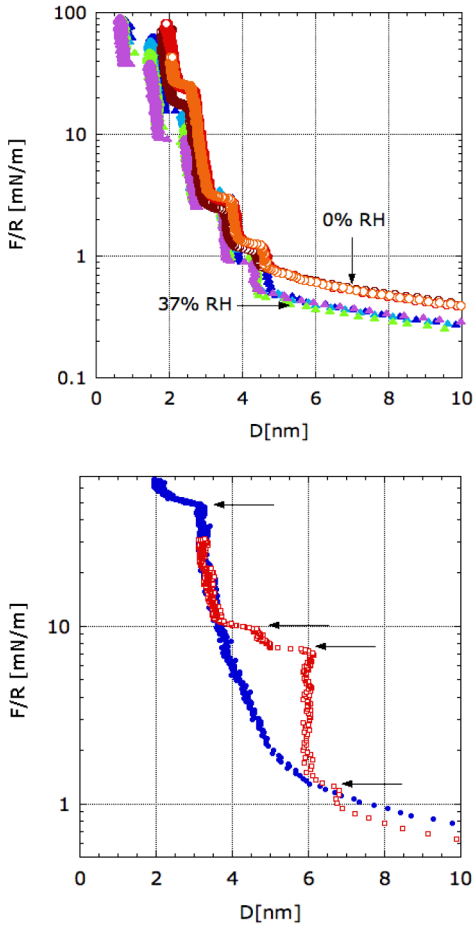

Figure 1. Top: Force isotherms between mica surfaces across [EMIM] FAP at 0 (empty circles) and 37% RH (full triangles). Bottom: Force isotherms between mica surfaces across [HMIM] FAP at 37% RH upon approach (full circles: no sliding; empty squares: continuous sliding).

37% RH during loading. The small long-range repulsion extends out to separations of 50 nm. Hydrodynamic drag does not account for the measured long-range repulsion (D > 5 nm). Instead, the force scales exponentially with D, in agreement with a double-layer repulsion corresponding to effective ion dissociation <0.02% (see details of calculation in SI). This model assumes the negative surface charge of mica; previous experiments have demonstrated the ion-exchange of K^+ on mica surfaces with imidazolium-based ILs.[25,26] The double-layer force and the low ion dissociation are in agreement with recent measurements.[13] The influence of the RH on the double-layer repulsion is negligible, considering the variations between force−distance curves obtained with different pairs of mica surfaces, especially at ambient RH, which is reflected in the large standard deviation of the fitting parameters. This has been classically attributed to the individual properties of the two mica sheets in the different experiments in previous SFA studies.

At D < 5 nm a short-range repulsion dominates, resulting from van der Waals forces, ion-surface binding forces, and forces induced by ion structuring. This leads to film-thickness transitions that are characteristic of a layer of ions being collectively squeezed out of the contact.[5−13] Thus, the nanoconfined films are ordered in layers. Higher RH leads to a smaller force required for each film-thickness transition to take place, as shown in Figure 1a, and strongly affects the dynamics of the measured transitions and, as discussed later, the film structure. Figure S3 (in the SI) shows representative curves for the time-dependent, film-thickness transitions. The layers slip up to 25 times faster (Figure S3c in the SI) if the mica surface is wetted by water, suggesting that either the shear plane must involve the interfacial water layer or water influences the film structure across the gap and as a result the resistance to squeeze-out/thin-out is reduced.

The average thickness of the layers under dry conditions is $\Delta = 5.4 \pm 0.5$ Å, while the last resolved layer is characteristically smaller, $\Delta \approx 4.2 \pm 0.2$ Å, which corresponds to the most strongly bound layer (Figure S4 in SI). Owing to the negative surface charge, the surface-adsorbed layers are enriched in cations. EMIM can readily incorporate the ethyl group into the first layer above the mica surface.[27] Due to the size of the imidazolium ring with extended ethyl along the surface,[9] cation crowding[28] is not very likely but rather either a surface-charge compensation through a single cation layer or overscreening.[29] The composition of further layers is unknown but is likely to consist of anions and cations, in contrast with the cation-rich surface-adsorbed layer, which agrees with the change of layer thickness. Both alternating cation and anion sublayers ("layer-by-layer") and checkerboard-like layers have been found experimentally on single surfaces,[30] but no experimental results are available for the confined IL film. A molecular-mechanics calculation was carried out with a MMFF94 force-field model (Avogadro software[31]), to determine the optimized geometry of the *isolated ions*, that is, neglecting any interaction between them or with the solid surface and neglecting the confining pressure. This calculation yields ~2.2 Å × 3.8 Å × 7.6 Å for $EMIM^+$ and ~4.2 Å × 6.5 Å × 7.46 Å for FAP^-. Assuming a layer-by-layer composition, the measured thickness of the dry layers is in best agreement with the ions lying with their largest dimension parallel to the surface and the shortest one perpendicular to the surface, leading to ~6.4 Å as the thickness for the layer-by-layer configuration—larger than the measured layer thickness. This estimation results from a highly simplified model because ions are not hard spheroids, and interactions between the ionic moieties lead to more effective ion packing, which is further enhanced by the confining pressure. These simplifications may explain the overestimation of the layer thickness.

At ambient RH, the average layer thickness is clearly larger and uniform across the gap, $\Delta = 7.1 \pm 0.2$ Å (see Figure S4 in the SI), more transitions are resolved, and the thickness of the boundary film[8] is smaller (1.8 ± 0.3 nm vs 1.0 ± 0.3 nm). Furthermore, the adhesion increases by a factor of 2 (see Figure S5 in SI), implying a strong change in surface energy of the system owing to surface-adsorbed water (differences of 50% are obtained between pairs of mica surfaces). This behavior is completely reversible after drying.

Despite the small amount of water absorbed by the bulk ILs, the concentration of water on mica surface is expected to be much higher under equilibrium conditions due to the hydrophilic surface properties. An accurate calculation is not possible without knowledge of partitioning coefficients, but

dx.doi.org/10.1021/jz402451v | J. Phys. Chem. Lett. 2014, 5, 179−184

surface concentration of water has been observed for OMCTS at different RHs.[32]

Our results indicate that the composition gradient of the layers across the gap vanishes in the presence of the interfacial layer. Surface-sensitive vibrational sum-frequency-generation spectroscopy has shown that interfacial water affects the ion-surface interaction via hydrogen bonding between surface water and imide-based IL-anions.[33] Similarly, hydrogen bonding between interfacial water and the phosphorus-based anion can be expected. This would lessen the cation surface concentration, substituting the well-accepted, cation-rich surface-adsorbed layer in the dry experiments, by a checkerboard-like adlayer, that is, adsorption of both anions and cations at the surface, with unknown relative concentrations. The same experimental technique has also shown that the imidazolium cation reorients with respect to the gas–liquid interface for hydrophobic anions when water is added, while the orientation in the hydrophilic liquid remains unaffected.[34] In agreement with this, the observed increase in layer thickness suggests that the ions reorient with the largest dimension (~7 Å) being perpendicular to the (wet) surface within all of the layers across the gap. Thus, changes of layer thickness and of adhesion can be explained through a change in ion–surface interaction and ion–pair orientation induced by surface-bound water (see possible configurations in ref 35).

Similar measurements do *not* show a *clear* layered structure for the nanoconfined [HMIM] FAP (except for a slow transition at F/R ≈ 50 mN/m, Figure 1b). The hexyl chains adopt an upright orientation[36] due to attractive lateral interactions between the hydrocarbon chains, promoting interlayer interdigitation[14] and disrupting the layered structure. In contrast, in force measurements between gold and a silica sphere[14] by AFM, layers of [HMIM] FAP were resolved, demonstrating the significant influence of the surface–IL interaction and confinement geometry on the film structure. Furthermore, if the surfaces are brought together while sliding, the layered structure of the [HMIM] FAP becomes more pronounced in the structural force (Figure 1b), indicating a shear-driven layering (10 ± 2 Å, in very good agreement with ref 14): the alkyl chains are combed as the surfaces pass each other, similar to the alignment of closely packed self-assembled monolayers during shear observed in simulations[37] and experiments with straight-chain and branched hydrocarbons.[38] The behavior is reversible. The influence of water on ion reorientation and ion-pair packing also depends on the length of the alkyl chains;[39] therefore, it can be expected to differ from that occurring with [EMIM] FAP. More details are provided below.

The lubrication performance is discussed next. Under both dry and ambient conditions, both ILs exhibit COF ≤ 0.015 before the last layer is squeezed out from the contact; that is, the friction is on the order of the instrumental resolution for films with thickness $D \geq 2$ nm.

Under dry conditions, the following friction sequence repeats during unidirectional sliding after the last layer of [EMIM] FAP is pushed out (Figure 2a): Initially friction increases, up to a yield point—eventually followed by a slow relaxation and again an increase in friction. The yield strength suggests the *solid-like* behavior of the boundary IL film. Then friction decreases abruptly within 0.5 s (collective slip) down to values of the order of magnitude of the instrument resolution. While friction increases, microstick-slip events are observed (see Figures S6a and S6b in the SI for details). During this nonperiodic stick–slip response, the film thickness variations are on the order of the instrument resolution. The maximum measured friction in the boundary film is 1.2 mN at a maximum load of 1.71 mN. In contrast, the resistance to shear of dry [HMIM] FAP remains very low over the whole range of applied loads (in Figure 2a, COF ≤ 0.015 for D = 1.3 nm). Complex friction response has been previously observed in SFA measurements (e.g., for squalane between mica surfaces): kinetic friction increased steadily over repetitive cycles and collapsed intermittently to the average value. Individual slip cycles also consisted of a cascade of smaller slip events,[16,17] indicating the presence of large domains or long-range cooperativity compared with the molecular dimensions in the film. Thus, it should be noted that the measured stick–slip response with an SFA results from multiple cooperative processes with different relaxation times taking place[40] within a large contact area (tens of square

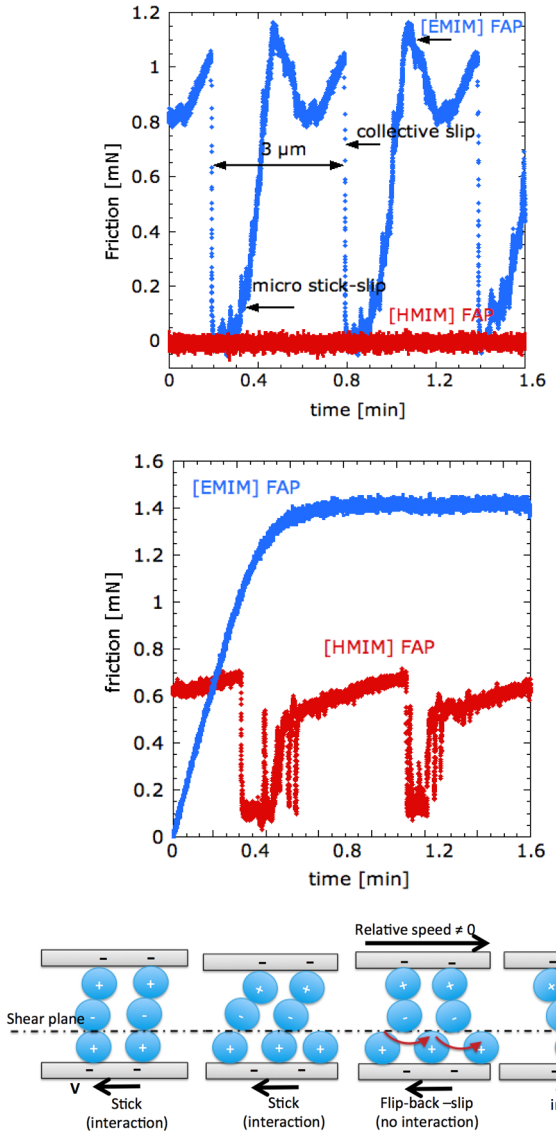

Figure 2. Friction force between mica surfaces in [EMIM] FAP and [HMIM] FAP (boundary films, load = 1.7 mN and 2.05, respectively) sliding at 0.1 μm/s over a distance of 10 μm under dry conditions (top) and at ambient RH (center). Bottom: Flip-flop model for a slip event; schematic representation of the IL structure under dry conditions.

dx.doi.org/10.1021/jz402451v | J. Phys. Chem. Lett. 2014, 5, 179–184

micrometers) and should not be confused with atomic stick–slip[41] described commonly by a Tomlinson-like model.

At ambient RH, the friction response of both boundary IL-films differs greatly. For [EMIM] FAP ($D \approx 0.8$ nm), after reaching the yield point (friction = 1.5 mN, load = 2 mN, COF ≈ 0.75), sliding is smooth, meaning that the critical speed for stick–slip initiation[38] in the presence of interfacial water is lower ($v_c < 0.1$ μm/s) than that under dry conditions ($v_c > 0.1$ μm/s). Although stick–slip vanishes, friction is high, as expected from the increase in adhesion (Figure S5 in the SI). Smooth sliding was also obtained for [EMIM] $EtSO_4$ at 37% RH (not shown) with a lower COF (in agreement with ref 9), although P_2O_5 was used in ref 9 as a drying agent. Indeed, stick–slip also has been observed to vanish if the strength of the interfacial interactions between Langmuir–Blodgett layers is low, which might be the case for water/[EMIM] $EtSO_4$ mixtures.[24] In contrast, the friction response of [HMIM] FAP consists of sequences with initial stick and superposed microstick-slips and larger slips. After the yield point is achieved, a collective slip leads to an abrupt reduction of friction (within 0.3 s) to nonmeasurable friction values. The maximum friction is 0.6 mN at a load of 2 mN.

While a decrease in the critical speed with increasing RH is observed for [EMIM] FAP, such a conclusion cannot be drawn for [HMIM] FAP because friction under dry conditions lies below the instrumental resolution, and therefore no information about the critical speed is available. But it is noted that the critical speed of [HMIM] FAP *at ambient RH* is higher than that for [EMIM] FAP because smooth sliding is observed for the latter. This is not a surprising result considering that interactions of imidazolium-based cations with anions do not scale monotonically with the alkyl chain length,[42] the tendency for tail aggregation increases with larger alkyl chain length,[43] and the nanostructures of precursor imidazolium-IL films with different alkyl chains are intrinsically different.[44]

The lubricating performance of [HMIM] FAP is better than that of [EMIM] FAP under both dry and wet conditions, which is consistent with the good lubricating properties of additives with long and branched chains.[17,38] The periodic stick–slip measured in ref 12 might result from the faster speeds (>0.5 μm/s) and much shorter sliding distance (500 nm) than that in our experiments, the different system dynamics, as well as the different IL composition. In fact, it has been demonstrated that the latter has a significant impact on the friction response measured by eSFA: while Perkin and coworkers showed periodic stick–slip response for 1-butyl-1-methylpyrrolidinium bis[(trifluoromethane)sulfonyl]imide in ref 12, they observed smooth sliding for [EMIM] $EtSO_4$ with the same experimental setup and under similar conditions.[9]

Knowing the lateral spring constant, the friction force can be converted into the real displacement of the upper surface (spring deflection). During a collective slip, the slip distance is ~0.26 μm for [HMIM] FAP and ~0.52 μm for [EMIM] FAP, and the corresponding speeds, ~0.867 and ~1.04 μm/s, are ~10× faster than the sliding speed of the lower surface. Microslips are ~1 order of magnitude slower than the collective slips (~0.1 μm/s for [HMIM] FAP and ~0.16 μm/s for [EMIM] FAP). Stick–slip has been classically considered to result from freezing (stick) –melting (slip) phase transitions or, more broadly, by a rearrangement of molecules in confinement[38] (melting is unlikely due to coulombic interactions between ions[12,45]).

Thus, we propose the slip events to be influenced by so-called 'flip-flops' (instead of by melting transitions), which are cooperative processes that result from interlayer (perhaps intralayer) ion correlations at the shear plane. In the selected ILs, ion correlations result from the interplay of Coulomb, van der Waals, and steric interactions. Our own synchrotron X-ray reflectivity measurements are still not conclusive regarding the composition of the layers across the confined film. However, we assume the IL-boundary layer to consist of alternating cation and anion sublayers,[9,35] the strongest interaction being between cation and surface, where the charge is localized, under the assumption that the mica surface is free of water and of organic contamination. Thus, the shear plane is probably located between the cation and anion sublayers. During stick, the lower surface moves laterally at 0.1 μm/s, while at the shear plane a cation sublayer coulombically interacts with the upper anion layer; the upper layers and the surface are pulled laterally, and ions reorient, rearrange, and realign ('flip' in the model), which leads to energy dissipation.[46] As soon as the yield point is reached, the upper layers flip back, releasing kinetic energy (up to 10 times faster than the velocity of the lower surface). This can happen locally, leading to microslips, or collectively over the contact area, leading to a collective slip, but in both cases leading to energy dissipation.[46] Friction reduces until the cation sublayer interacts with the oncoming anion at the shear plane and they stick together again (the lower surface has moved effectively 30–50 nm during a collective slip at a constant speed of 0.1 μm/s).

The flip-flop picture is consistent with Schallamach's model,[47] which describes sliding as a result of incoherent shearing and reformation of nanodomains or 'junctions', as a rubber surface moves against its counter-surface. Each nanodomain is stretched until it breaks due to either thermal excitation or external force. This explanation is also accord with Drummond's energy-dissipation model for weakly adhering surfactant-bearing surfaces.[48] The observed slow friction variations during the stick phase (Figure 2a) might be related to rearrangements of ions/ion pairs taking place only in discrete domains within the contact. The negligible friction in films thicker than 2 nm is attributed to the presence of a shear plane with a certain degree of disorder, that is, liquid-like behavior.

Interfacial water contributes to the friction response. The ion-pair orientation is affected by the presence of water; therefore, the intralayer interactions at the shear plane are modified. Water, as with other contaminant molecule or solutes, can influence the ion-pair coordination, either promoting or hindering the ease with which the ions/alkyl chains can align parallel to the sliding direction, which in turn also influences interlayer interactions at the shear plane. Because there is an increase in friction with RH, bond formation (rather than rupture) is enhanced by water during sliding, according to Schallamach's and Drummond's picture.

Local slips in the contact region (microslips) always precede the occurrence of a large or collective slip. This has been observed in simulations[49] of granular media that mimic fault gauges in earthquake dynamics. Experiments have also shown that crack-like fronts at the interface of two plexiglass surfaces prior to sliding propagate at three different speeds, leading to different detachment processes or slips.[50] Microslips can be related to transitions of metastable 2D-domains, with size-dependent relaxation times. They nucleate and grow (microstick) or disappear (microslip), leading to a chaotic stick–slip response. If many of them occur, they can trigger a collective

dx.doi.org/10.1021/jz402451v | J. Phys. Chem. Lett. 2014, 5, 179–184

slip or 'avalanche',[19] which is accompanied by a large energy release and corresponds to a significant reorganization, in terms of contacts and contact forces.[49] Interestingly, this has been identified to be analogous to the coordinated multicellular movement of *M. xanthus* bacteria and in lubrication with branched hydrocarbons,[17] demonstrating that crackling noise behavior scales over many orders of magnitude.[19] We observe some differences in the measured sequences obtained with different pairs of mica surfaces. This has been attributed to the different angles between the surface lattices of the two mica sheets and the different sliding directions relative to these lattices in the different experiments in previous studies. Future modeling of the friction data (slip statistics) in terms of crackling-noise behavior will provide a better understanding about the (multiple) relaxation mechanisms during the stick–slip response.

In summary, when exposed to 37% RH, surface-adsorbed water modifies the ion-pair orientation of nanoconfined hydrophobic imidazolium ILs. This results in an increase in adhesion and worsening of lubricating performance of 1 to 2 nm IL films. The hexyl chain promotes lower friction compared with the ethyl chain. At speeds below the critical speed, interlayer ion interactions (mainly coulombic) during shear induce microslip events and collective slips or avalanches that abruptly decrease friction. The measured chaotic stick–slip friction response is reminiscent of crackling-noise systems. In analogy to these systems, we infer that ion (pair) packing and morphology, as well as shear speed, influence the friction response. This should be taken into account in the design of ILs with good lubricant properties for specific applications.

■ ASSOCIATED CONTENT

Supporting Information

Experimental method, optimized geometry of selected ions, calculation of double-layer repulsion, dynamics of film thickness transitions, size of layers in confined [EMIM] FAP, pull-off forces between mica surfaces in [EMIM] FAP, and details of microslips. This material is available free of charge via the Internet at http://pubs.acs.org.

■ AUTHOR INFORMATION

Corresponding Author

*E-mail: nspencer@ethz.ch.

Present Address

[§]R.M.E.-M.: Lab. for Smart Interfaces in Environmental Nanotechnology, Dept. of Civil and Environmental Engineering, University of Illinois at Urbana–Champaign, Urbana, Illinois 61801, United States.

Notes

The authors declare no competing financial interest.

■ ACKNOWLEDGMENTS

We are very grateful to Prof. Karin Dahmen, University of Illinois at Urbana–Champaign, and to Dr. Michele Griffa, EMPA, Switzerland, for useful discussions. We thank the Swiss National Science Foundation for financial support.

■ REFERENCES

(1) Armand, M.; Endres, F.; MacFarlane, D. R.; Ohno, H.; Scrosati, B. Ionic-Liquid Materials for the Electrochemical Challenges of the Future. *Nat. Mater.* **2009**, *8*, 621–629.

(2) Liu, H. T.; Liu, Y.; Li, J. H. Ionic Liquids in Surface Electrochemistry. *Phys. Chem. Chem. Phys.* **2010**, *12*, 1685–1697.

(3) Weingaertner, H. Understanding Ionic Liquids at the Molecular Level: Facts, Problems, and Controversies. *Angew. Chem., Int. Ed.* **2008**, *47*, 654–670.

(4) Greaves, T. L.; Drummond, C. J. Ionic Liquids as Amphiphile Self-Assembly Media. *Chem. Soc. Rev.* **2008**, *37*, 1709–1726.

(5) Horn, R. G.; Evans, D. F.; Ninham, B. W. Double-Layer and Solvation Forces Measured in a Molten-Salt and Its Mixtures with Water. *J. Phys. Chem.* **1988**, *92*, 3531–3537.

(6) Atkin, R.; Warr, G. G. Structure in Confined Room-Temperature Ionic Liquids. *J. Phys. Chem. C* **2007**, *111*, 5162–5168.

(7) Werzer, O.; Atkin, R. Interactions of Adsorbed Poly(Ethylene Oxide) Mushrooms with a Bare Silica-Ionic Liquid Interface. *Phys. Chem. Chem. Phys.* **2011**, *13*, 13479–13485.

(8) Li, H.; Rutland, M. W.; Atkin, R. Ionic Liquid Lubrication: Influence of Ion Structure, Surface Potential and Sliding Velocity. *Phys. Chem. Chem. Phys.* **2013**, *15*, 14616–14623.

(9) Perkin, S.; Albrecht, T.; Klein, J. Layering and Shear Properties of an Ionic Liquid, 1-Ethyl-3-Methylimidazolium Ethylsulfate, Confined to Nano-Films between Mica Surfaces. *Phys. Chem. Chem. Phys.* **2010**, *12*, 1243–1247.

(10) Perkin, S.; Crowhurst, L.; Niedermeyer, H.; Welton, T.; Smith, A. M.; Gosvami, N. N. Self-Assembly in the Electrical Double Layer of Ionic Liquids. *Chem. Commun.* **2011**, *47*, 6572–6574.

(11) Perkin, S. Ionic Liquids in Confined Geometries. *Phys. Chem. Chem. Phys.* **2012**, *14*, 5052–5062.

(12) Smith, A. M.; Lovelock, K. R. J.; Gosvami, N. N.; Welton, T.; Perkin, S. Quantized Friction across Ionic Liquid Thin Films. *Phys. Chem. Chem. Phys.* **2013**, *15*, 15317–15320.

(13) Gebbie, M. A.; Valtiner, M.; Banquy, X.; Fox, E. T.; Henderson, W. A.; Israelachvili, J. N. Ionic Liquids Behave as Dilute Electrolyte Solutions. *Proc. Natl. Acad. Sci. U.S.A.* **2013**, *110*, 9674–9679.

(14) Li, H.; Endres, F.; Atkin, R. Effect of Alkyl Chain Length and Anion Species on the Interfacial Nanostructure of Ionic Liquids at the Au(111)-Ionic Liquid Interface as a Function of Potential. *Phys. Chem. Chem. Phys.* **2013**, *15*, 14624–14633.

(15) Vanalsten, J.; Granick, S. The Origin of Static Friction in Ultrathin Liquid-Films. *Langmuir* **1990**, *6*, 876–880.

(16) Demirel, A. L.; Granick, S. Friction Fluctuations and Friction Memory in Stick-Slip Motion. *Phys. Rev. Lett.* **1996**, *77*, 4330–4333.

(17) Drummond, C.; Israelachvili, J. Dynamic Phase Transitions in Confined Lubricant Fluids under Shear. *Phys. Rev. E* **2001**, *63*, 041506–041517.

(18) Drummond, C.; Elezgaray, J.; Richetti, P. Behavior of Adhesive Boundary Lubricated Surfaces under Shear: A New Dynamic Transition. *Europhys. Lett.* **2002**, *58*, 503–509.

(19) Gibiansky, M. L.; Hu, W.; Dahmen, K. A.; Shi, W. Y.; Wong, G. C. L. Earthquake-Like Dynamics in Myxococcus Xanthus Social Motility. *Proc. Natl. Acad. Sci. U.S.A.* **2013**, *110*, 2330–2335.

(20) Sethna, J. P.; Dahmen, K. A.; Myers, C. R. Crackling Noise. *Nature* **2001**, *410*, 242–250.

(21) Israelachvili, J. N.; Tabor, D. The Measurement of Van Der Waals Dispersion Forces in the Range 1.5 to 130 Nm. *Proc. R. Soc. London, Ser. A* **1972**, *331*, 19–38.

(22) Israelachvili, J. N. Thin Film Studies Using Multiple-Beam Interferometry. *J. Colloid Interface Sci.* **1973**, *44*, 259–272.

(23) Heuberger, M. The Extended Surface Forces Apparatus. Part I. Fast Spectral Correlation Interferometry. *Rev. Sci. Instrum.* **2001**, *72*, 1700–1707.

(24) Balmer, T. E.; Christenson, H. K.; Spencer, N. D.; Heuberger, M. The Effect of Surface Ions on Water Adsorption to Mica. *Langmuir* **2007**, *24*, 1566–1569.

(25) Cipriano, B. H.; Raghavan, S. R.; McGuiggan, P. M. Surface Tension and Contact Angle Measurements of a Hexadecyl Imidazolium Surfactant Adsorbed on a Clay Surface. *Colloid Surf., A* **2005**, *262*, 8–13.

(26) Zhou, H.; Rouha, M.; Feng, G.; Lee, S. S.; Docherty, H.; Fenter, P.; Cummings, P. T.; Fulvio, P. F.; Dai, S.; McDonough, J.; et al.

Nanoscale Perturbations of Room Temperature Ionic Liquid Structure at Charged and Uncharged Interfaces. *ACS Nano* **2012**, *6*, 9818−9827.
(27) Segura, J. J.; Elbourne, A.; Wanless, E. J.; Warr, G. G.; Voitchovsky, K.; Atkin, R. Adsorbed and near Surface Structure of Ionic Liquids at a Solid Interface. *Phys. Chem. Chem. Phys.* **2013**, *15*, 3320−3328.
(28) Bazant, M. Z.; Storey, B. D.; Kornyshev, A. A. Double Layer in Ionic Liquids: Overscreening Versus Crowding. *Phys. Rev. Lett.* **2011**, *106*, 046102−046105.
(29) Simon, P.; Gogotsi, Y. Capacitive Energy Storage in Nanostructured Carbon-Electrolyte Systems. *Acc. Chem. Res.* **2013**, *46*, 1094−1103.
(30) Cremer, T.; Stark, M.; Deyko, A.; Steinruck, H. P.; Maier, F. Liquid/Solid Interface of Ultrathin Ionic Liquid Films: [C(1)C(1)-Lm][Tf2n] and [C(8)C(1)Im][Tf2n) on Au(111). *Langmuir* **2011**, *27*, 3662−3671.
(31) Hanwell, M. D.; Curtis, D. E.; Lonie, D. C.; Vandermeersch, T.; Zurek, E.; Hutchison, G. R. Avogadro: An Advanced Semantic Chemical Editor, Visualization, and Analysis Platform. *J. Cheminf.* **2012**, *4*, 1−17.
(32) Balmer, T. *Resolving Structural and Dynamical Properties in Nano-Confined Fluids*; ETH Zurich: Zurich, 2007.
(33) Fitchett, B. A.; Conboy, J. C. Structure of the Room-Temperature Ionic Liquid/Sio2 Interface Studied by Sum-Frequency Vibrational Spectroscopy. *J. Phys. Chem. B* **2004**, *108*, 20255−20262.
(34) Rivera-Rubero, S.; Baldelli, S. Influence of Water on the Surface of Hydrophilic and Hydrophobic Room-Temperature Ionic Liquids. *J. Am. Chem. Soc.* **2004**, *126*, 11788−11789.
(35) Mezger, M.; Schroder, H.; Reichert, H.; Schramm, S.; Okasinski, J. S.; Schoder, S.; Honkimaki, V.; Deutsch, M.; Ocko, B. M.; Ralston, J.; et al. Molecular Layering of Fluorinated Ionic Liquids at a Charged Sapphire (0001). *Surf. Sci.* **2008**, *322*, 424−428.
(36) Rollins, J. B.; Fitchett, B. D.; Conboy, J. C. Structure and Orientation of the Imidazolium Cation at the Room-Temperature Ionic Liquid/Sio2 Interface Measured by Sum-Frequency Vibrational Spectroscopy. *J. Phys. Chem. B* **2007**, *111*, 4990−4999.
(37) Mikulski, P. T.; Gao, G.; Chateauneuf, G. M.; Harrison, J. A. Contact Forces at the Sliding Interface: Mixed Versus Pure Model Alkane Monolayers. *J. Chem. Phys.* **2005**, *122*, 024701−024710.
(38) Gee, M. L.; Mcguiggan, P. M.; Israelachvili, J. N.; Homola, A. M. Liquid to Solid-Like Transitions of Molecularly Thin-Films under Shear. *J. Chem. Phys.* **1990**, *93*, 1895−1906.
(39) Schenk, J.; Panne, U.; Albrecht, M. Interaction of Levitated Ionic Liquid Droplets with Water. *J. Phys. Chem. B* **2012**, *116*, 14171−14177.
(40) Drummond, C.; Israelachvili, J. Dynamic Behavior of Confined Branched Hydrocarbon Lubricant Fluids under Shear. *Macromolecules* **2000**, *33*, 4910−4920.
(41) Luthi, R.; Meyer, E.; Bammerlin, M.; Howald, L.; Haefke, H.; Lehmann, T.; Loppacher, C.; Guntherodt, H. J.; Gyalog, T.; Thomas, H. Friction on the Atomic Scale: An Ultrahigh Vacuum Atomic Force Microscopy Study on Ionic Crystals. *J. Vac. Sci. Technol., B* **1996**, *14*, 1280−1284.
(42) Lockett, V.; Sedev, R.; Ralston, J.; Horne, M.; Rodopoulos, T. Differential Capacitance of the Electrical Double Layer in Imidazolium-Based Ionic Liquids: Influence of Potential, Cation Size, and Temperature. *J. Phys. Chem. C* **2008**, *112*, 7486−7495.
(43) Binetti, E.; Panniello, A.; Triggiani, L.; Tommasi, R.; Agostiano, A.; Curri, M. L.; Striccoli, M. Spectroscopic Study on Imidazolium-Based Ionic Liquids: Effect of Alkyl Chain Length and Anion. *J. Phys. Chem. B* **2012**, *116*, 3512−3518.
(44) Beattie, D. A.; Espinosa-Marzal, R. M.; Ho, T. T. M.; Popescu, M. N.; Ralston, J.; Richard, C. J. E.; Sellapperumage, P. M. F.; Krasowska, M. Molecularly-Thin Precursor Films of Imidazolium-Based Ionic Liquids on Mica. *J. Phys. Chem. C* **2013**, *117*, 23676−23684.
(45) Lei, Y.; Leng, Y. Stick-Slip Friction and Energy Dissipation in Boundary Lubrication. *Phys. Rev. Lett.* **2011**, *107*, 47801−47805.
(46) Israelachvili, J. Adhesion, Friction and Lubrication of Molecularly Smooth Surfaces. In *Fundamentals of Friction: Macroscopic and Microscopic Processes*, Singer, I. L., Pollock, H. M., Eds.; Springer Netherlands: The Netherlands, 1992; Vol. *220*, pp 351−385.
(47) Schallamach, A. How Does Rubber Slide. *Wear* **1971**, *17*, 301−312.
(48) Drummond, C.; Israelachvili, J.; Richetti, P. Friction between Two Weakly Adhering Boundary Lubricated Surfaces in Water. *Phys. Rev. E* **2003**, *67*, 066110−066126.
(49) Ferdowsi, B.; Griffa, M.; Guyer, R. A.; Johnson, P. A.; Marone, C.; Carmeliet, J. Microslips as Precursors of Large Slip Events in the Stick-Slip Dynamics of Sheared Granular Layers: A Discrete Element Model Analysis. *Geophys. Res. Lett.* **2013**, *40*, 4194−4198.
(50) Rubinstein, S. M.; Cohen, G.; Fineberg, J. Detachment Fronts and the Onset of Dynamic Friction. *Nature* **2004**, *430*, 1005−1009.